

## BASIC – ALIMENTARY TRACT

# Targeted Expression of Oncogenic K-ras in Intestinal Epithelium Causes Spontaneous Tumorigenesis in Mice

KLAUS-PETER JANSSEN,\* FATIMA EL MARJOU,\* DANIEL PINTO,† XAVIER SASTRE,§  
DANY ROUILLARD,|| CORALIE FOUQUET,¶ THIERRY SOUSSI,¶ DANIEL LOUVARD,\* and  
SYLVIE ROBINE\*

\*Cellular Morphogenesis and Signalisation, UMR144, Institut Curie, Paris; †Department of Immunology, UMC, Utrecht, The Netherlands;

§Service d'Anatomo-pathologie, Institut Curie, Paris; ||Service de Cytopathologie et Cytométrie Clinique, Institut Curie, Paris; and

¶Laboratoire de Génomotoxicologie des Tumeurs, Institut Curie, Paris, France

**Background & Aims:** Ras oncoproteins are mutated in about 50% of human colorectal cancers, but their precise role in tumor initiation or progression is still unclear. **Methods:** This study presents transgenic mice that express K-ras<sup>V12G</sup>, the most frequent oncogenic mutation in human tumors, under control of the murine villin promoter in epithelial cells of the large and small intestine. **Results:** More than 80% of the transgenic animals displayed single or multiple intestinal lesions, ranging from aberrant crypt foci (ACF) to invasive adenocarcinomas. Expression of K-ras<sup>V12G</sup> caused activation of the MAP kinase cascade, and the tumors were frequently characterized by deregulated cellular proliferation. Unexpectedly, we obtained no evidence of inactivating mutations of the tumor suppressor gene *Apc*, the “gate-keeper” in colonic epithelial proliferation. However, spontaneous mutation of the tumor-suppressor gene *p53*, a frequent feature in the human disease, was found in 3 of 7 tumors that were tested. **Conclusions:** This animal model recapitulates the stages of tumor progression as well as a part of the genetic alterations found in human colorectal cancer. Furthermore, it indicates that activation of K-ras in concert with mutations in *p53* may constitute a route to digestive tumor formation and growth, underlining the fact that the pathway to intestinal cancer is not necessarily a single road.

Cancers of the colon and rectum are among the most frequent tumors in Europe and North America. More than 50% of the population develop a colorectal tumor by the age of 70 years, which progresses to malignancy in 10% of the cases.<sup>1</sup> Several attempts have been made to obtain murine models to study the formation and growth of tumors in the intestinal tract.<sup>2</sup> The understanding of the function of several tumor suppressor genes in the development of colorectal cancer has benefited from mouse models, e.g., in the case of *APC* and the

Wnt signaling cascade,<sup>3–5</sup> the same holds true for the involvement of the mismatch repair machinery in carcinogenesis.<sup>6,7</sup> Inactivation of the murine gene *SMAD3*, a mediator of transforming growth factor  $\beta$  signaling, resulted in colorectal cancer,<sup>8</sup> whereas the tumorigenic effects of a deletion of the catalytic subunit of phosphoinositide-3 kinase are currently under debate.<sup>9,10</sup> However, modeling the role of oncogenes, in particular K-ras<sup>V12G</sup>, the most frequently mutated oncogene in colorectal cancer, has only been partially successful.<sup>2,11,12</sup> Ras proteins are small GTPases that are mutated in about 30% of all human tumors and in 50% of human colorectal cancers.<sup>13–16</sup> The mammalian Ras protein family comprises several isoforms (*H-ras*, *N-ras*, and *K-ras*) with high degrees of sequence identity that are all able to cycle between an active guanosine triphosphate (GTP)-bound conformation and an inactive guanosine diphosphate (GDP)-bound form. The Ras signaling cascade constitutes a major genetic pathway controlling cell proliferation and apoptosis, and Ras proteins are able to integrate extracellular signals from diverse receptor types. Among their multiple effectors, the best studied are Raf-1 and the MAP kinase cascade, as well as phosphoinositide-3 kinase and Akt/PKB.<sup>16–19</sup> Transgenic expression of K-ras<sup>V12G</sup> in postmitotic villus enterocytes caused intestinal dysplasia, but the authors did not observe any neoplasms.<sup>11,20</sup> They explained this finding by the short residence time of migrating enterocytes on the villus, which is not sufficient to allow clonal expansion. In a

**Abbreviations used in this paper:** ACF, aberrant crypt foci; APC, adenomatous polyposis coli; GDP, guanosine diphosphate; GTP, guanosine triphosphate; LOH, loss of heterozygosity; MAPK, mitogen-activated protein kinase; PCR, polymerase chain reaction.

© 2002 by the American Gastroenterological Association

0016-5085/02/\$35.00

doi:10.1053/gast.2002.34786

recent publication, Johnson et al.<sup>12</sup> demonstrated an elegant mouse model for Ras-dependent carcinogenesis that is based upon spontaneous recombination events in the whole animal. Although the transgenic mice failed to develop intestinal tumors, they showed a high predisposition for lung cancer and other tumor types. According to the authors, this may be because of tissue-specific differences in the frequency of recombination events or because of the relative order of *ras* mutations in the tumorigenic process. Activating *K-ras* mutations are associated with early to intermediate stages of the multi-step neoplastic process, but it is believed that their tumorigenic effects develop in the context of a preexisting *APC* gene mutation.<sup>15,21</sup> To address the question of whether activated Ras oncoproteins are able to induce intestinal tumors or depend on previous mutations of the tumor suppressor gene *APC*, we have generated a new transgenic mouse model that expresses human *K-ras*<sup>V12G</sup> under control of the murine villin promoter in epithelial cells of the large and small intestine. This promoter has been shown to target expression of transgenes in stem cells, which remain anchored in the crypt during the normal renewal process of the intestinal mucosa.<sup>22,23</sup> Furthermore, this cell type goes through several cycles of cell division, which is necessary to accumulate somatic mutations that are required for tumorigenesis.

## Materials and Methods

### Establishment of the Transgene and Transgenic Mouse Lines

The vector pCEX-V3-V12-K-*ras* was generously provided by Dr. J. De Gunzburg (Inst. Curie, Paris, France). It contains the coding sequence of human *K-ras*4B with an activating glycine to valine mutation at codon 12 (V12G).<sup>24</sup> We modified the *K-ras* coding sequence by polymerase chain reaction (PCR) with sequence-specific primers that introduced a *ScaI* site at the 5' end and a *NotI* site at the 3' end (sense: 5'-TGCAAAAGTACTGAATATAAACTTGTG-3', antisense: 5'-ATTTGCGGCCGCTTTACATAATTACACT-3'). PCR was carried out with the Expand High Fidelity System (Boehringer Mannheim, Indianapolis, IN). The resulting *ScaI/NotI* fragment with a size of 580 bp was ligated into the p9kb-*AatII* vector, a plasmid based on the pBluescript II KS vector (Stratagene, La Jolla, CA) that contains a 9-kb region from the murine villin gene, followed by an *AatII/NotI* at its 5' side. This construct was digested with *NotI*, and the cohesive ends were blunted with Klenow enzyme. In the next step, the human growth hormone polyadenylation sequence (HGH) from the expression plasmid pCB6<sup>25</sup> was added to this construct. PCR was carried out on pCB6 with primers that introduced *SmaI* sites at both ends of the polyadenylation sequence and a single *NotI* site at the 3' end for linearization of the plasmid (sense: 5'-TCCCCCGGGTGGCATCCCT-

GTGACC-3', antisense: 5'-TCCCCCGGGGCGGCCGC-CAATTC AACAGGCATC-3'). The resulting 640-bp PCR fragment was digested with *SmaI* and ligated into the p9kb-*AatII-K-ras* plasmid to obtain the final targeting construct. After confirming this vector by sequencing, a linear *NotI/KpnI* DNA fragment of this plasmid without vector sequences was purified with Elutip D columns (Schleicher & Schuell, Keene, NH). Pronucleus DNA injections and embryo transfers were carried out according to standard procedures. The hybrid line B6D2 (C57Bl/6 × DBA/2) was used as embryo donor and recipient. Germline transmission was detected by Southern blot or PCR analysis of tail DNA obtained at weaning. Transgenics were maintained by crosses to B6D2 littermates.

### Western Blots

Equal amounts of protein were separated on 13% polyacrylamide gels<sup>26</sup> and further subjected to immunoblotting<sup>27</sup> following standard procedures. The immunoreactive bands were detected using the primary antibodies indicated: horseradish peroxidase-conjugated goat anti-mouse IgG, goat anti-rabbit IgG, and goat anti-hamster IgG as secondary antibodies (Jackson ImmunoResearch, West Grove, PA), visualized with an enhanced chemiluminescence substrate detection kit (Pierce, Rockford, IL). The antibodies used were the following: anti-Villin ID2C3,<sup>28</sup> anti-pan-Ras (Transduction Laboratories, Lexington, KY), anti-β-Actin (Sigma, St. Quentin, France), anti-Bcl2 (PharMingen Becton Dickinson), anti-phospho-(Thr202, Tyr204)-p44/42 mitogen-activated protein kinase (MAPK), anti-p44/42 MAPK, anti-phospho-(Thr308)-Akt, anti-phospho-(Ser473)-Akt, and anti-Akt (all from New England Biolabs, Beverly, MA).

### GTP-Ras Pulldown Assay

Snap-frozen bacterial lysates containing recombinant glutathion-S-transferase-RalGDS (GST-RalGDS) fusion protein in preparation buffer [phosphate-buffered saline (PBS) substituted with 0.5 mmol/L DTT, 1 mmol/L PMSF, 1 μmol/L aprotinin, 10 μmol/L leupeptin, and 1% Triton X-100] were obtained from G. Gaudriault (Inst. Curie). One aliquot (1.4 mL) of bacterial lysate was mixed with 200 μL of a 50% (vol/vol) slurry of Glutathione Sepharose 4B (Amersham Pharmacia) that had previously been washed twice with PBS and twice with tissue lysis buffer (see below) and incubated at 4°C for 60 minutes. After centrifugation, the supernatant was removed and the resin washed 3 times with 10-bed volumes of tissue lysis buffer. Snap-frozen mouse tissue was directly lysed in ice-cold tissue lysis buffer (50 mmol/L Tris-HCl, pH 7.5, 150 mmol/L NaCl, 20 mmol/L MgCl<sub>2</sub>, 5 mmol/L EGTA, 1% Triton X-100, 1% NP-40, 1 mmol/L benzamidine, 1 mmol/L PMSF, Mammalian Protease Inhibitor Cocktail; Sigma) using a 1 mL Dounce Homogenizer. The homogenates were incubated for 10 minutes at 4°C, and, after centrifugation (15,000g, 15 minutes, 4°C), the cleared supernatants were collected. The protein concentration was determined using a Bio-Rad assay (BioRad, Richmond, CA). Equal amounts of protein (1.5 to 2 mg in total) were incubated in a

total volume of 600  $\mu$ L with 30  $\mu$ L glutathion-sepharose beads that had previously been coupled to the recombinant GST-RalGDS. The mixture was incubated at 4°C for 2 hours on a wheel and centrifuged (15,000g, 5 minutes, 4°C), and the resulting pellet was washed 3 times with tissue lysis buffer. The pellets were resuspended in Laemmli-sample buffer, subjected to SDS-PAGE, and subsequently transferred to nitrocellulose membranes.

### Molecular Biological Methods

DNA was extracted from mouse tails in lysis buffer (50 mmol/L Tris/HCl, pH 7.5, 0.1 mol/L NaCl, 0.5% SDS, 5 mmol/L EDTA, 100  $\mu$ g/mL proteinase K), transferred onto nitrocellulose membranes for Southern blot analysis (Schleicher & Schuell), and incubated with <sup>32</sup>P-labeled probes generated using a random prime labeling kit (Stratagene). Hybridization was performed at 37°C for 12–16 hours in hybridization buffer containing 50% formamide and 2 $\times$  SSC. The blots were washed twice for 5 minutes in 2 $\times$  SSC containing 0.1% SDS at 37°C and for 60 minutes in a buffer containing 50% formamide and 2 $\times$  SSC at 37°C. RNA was extracted from different tissues using the RNA Now Kit (Ozyme, St. Quentin, France). Reverse transcription PCR analysis was performed as described.<sup>23</sup> The primers used were the following: sense villin (5'-CAAGCCTGGCTCGACGGCC-3'), and Ras antisense (5'-ATTTGCGGCCGCTTACATA-ATTACAACT-3'), generating a 400-bp product.

### Tumor Analysis and Processing of Tissue

Animals were killed at the ages indicated or when they showed signs of distress, and the gross study of the tissues was performed as described.<sup>29</sup> Briefly, the entire intestine was removed and opened longitudinally, sections of approximately 10-cm length were spread out on filter paper (Drying Block, Schleicher & Schuell), fixed overnight at 4°C in NoTox fixative (Earth Safe Industries, Inc., Bellemead, NJ), and finally transferred to 70% ethanol. The size and location of macroscopically visible tumors were determined, followed by resection and embedding of lesions in paraffin according to standard procedures. Tumors were classified according to standard histopathological criteria. In addition, a number of freshly isolated tumors were snap-frozen in liquid nitrogen and stored at -80°C. The frozen tumors were either used for DNA/RNA extraction (Qiagen RNA/DNA Kit), or embedded in Tissutek OCT compound (Sakura B.V., Zoeterwoude, The Netherlands) and processed for cryosections. Kidneys, liver, and lungs of all animals were investigated for the presence of metastases by macroscopic analysis, and, in a number of cases, microscopic analysis of serial H&E-stained sections. For protein analysis, snap-frozen mouse tissue or scrapings of intestinal mucosa were lysed in ice-cold lysis buffer (50 mmol/L Tris-HCl, pH 7.5, 150 mmol/L NaCl, 1 mmol/L benzamidine, 1 mmol/L PMSF, 1 mmol/L DTT, 2 mmol/L EGTA, 1% Triton X-100, 1% NP-40, Mammalian Protease Inhibitor Cocktail; Sigma), using a 1 mL Dounce Homogenizer. After centrifugation (15,000g, 15 minutes, 4°C), the supernatants were collected.

The protein concentration was determined using a Bio-Rad assay (Bio-Rad), with bovine serum albumin as standard. Analysis of the colon for aberrant crypt foci (ACF) was performed essentially as described.<sup>30</sup> Briefly, segments of the colon were pinned out flat and fixed as described previously. The fixed tissue was stained for 1 minute in 0.2% methylene blue (Sigma) in PBS and rinsed in fresh phosphate buffer at 4°C for 2 hours. The tissue segments were placed luminal side up on microscope slides and observed with a low-magnification lens. All crypts identified as aberrant were at least 3 times larger in diameter than normal crypts, and their lumina were mostly oval or elongated rather than circular.

### Histopathology

Intestinal specimens were processed immediately after killing the animal. Small and large intestines were opened longitudinally, and tumorous regions were dissected together with surrounding normal tissue and fixed in AFA (75% ethanol, 20% formalin, and 5% acetic acid) for 24 hours. After embedding, 3- $\mu$ m-thick sections were cut from the tissue blocks, dewaxed, rehydrated, and processed by routine H&E staining. All the lesions were reviewed by a single, experienced pathologist (X.S.). Tumors were classified and graded according to the World Health Organization classification of tumors.<sup>31</sup> Adenocarcinomas were considered invasive if malignant epithelial cells, arranged in glandular and/or trabecular structures, were found invading at least the submucosa.

### Flow Cytometry

Two transgenic mice and 2 control animals were injected IP with 0.01 mL per 1-g animal body weight of a 6 mg/mL solution of 5-bromo-2'-deoxyuridine (BrdU; Sigma; 60 mg/kg body weight). The animals were killed 2 hours after the injection; the entire intestine was removed and opened longitudinally. Control tissue and tumors were dissected under a binocular and fixed overnight in 70% ethanol at 4°C. Nuclear suspensions were prepared by mincing the tissue in 0.1 N HCl solution containing 0.04% pepsin, then incubation at 37°C for 60 minutes. Release of nuclei was controlled at 20-minute intervals by trypan blue staining using a light microscope. The resulting solution was filtered through a 0.35- $\mu$ m membrane, spun for 5 minutes at 1400 rpm, and resuspended in 1.5 mL of a 2 N HCl solution for 20 minutes at 37°C. The solution was neutralized by the addition of 3 mL PBT (PBS containing 0.5% BSA, 0.5% Tween 20) and centrifuged at 1400 rpm for 5 minutes. The nuclei were resuspended in PBT at a concentration of 2  $\times$  10<sup>6</sup> nuclei per mL and stained with a monoclonal rat anti-BrdU antibody (Harlan Sera-Lab, Belton, United Kingdom) diluted at 1:25 for 60 minutes at room temperature. The nuclei were subsequently washed once in PBT and incubated with FITC-coupled goat-anti-rat IgG (Jackson Immunoresearch) at a concentration of 10  $\mu$ g/mL in PBT at room temperature for 45 minutes in the dark. After washing with PBT, the nuclear suspension was resuspended at 10<sup>6</sup> nuclei per mL in PBS containing 10  $\mu$ g/mL propidium iodide. Bivariate distributions of BrdU content

(FITC) vs. DNA content (propidium iodide) were measured using a FACScan flow cytometer (Becton Dickinson, San Jose, CA). Doublets and clumps were excluded from the analysis by gating on a bivariate distribution of the propidium iodide area vs. signal width.

### Immunofluorescence on Tissue Sections

Cryosections of Tissue-tek OCT (Sakura) embedded mouse tissues were cut at 5- $\mu$ m thickness, air dried and fixed with either 3% paraformaldehyde at room temperature for 20 minutes or with methanol at  $-20^{\circ}\text{C}$  for 10 minutes. The paraformaldehyde-fixed sections were treated with 50 mmol/L  $\text{NH}_4\text{Cl}$  in PBS for 20 minutes and solubilized with 0.1% Triton X-100 for 5 minutes. Antibodies used were the following: mAb anti-Villin ID2C3,<sup>28</sup> anti-Ki67 pAb (Novocastra), and anti- $\beta$ -catenin mAb M5.2 (monoclonal antibody directed against recombinant human  $\beta$ -catenin, manuscript in preparation); secondary antibodies were goat anti-mouse IgG and goat anti-rabbit IgG coupled to Alexa488 or Cy3 (Jackson ImmunoResearch), TRITC-phalloidin (Sigma) to visualize actin and the dye Hoechst 33258 (Sigma) to stain nuclei.

### Loss of Heterozygosity Analysis

Loss of heterozygosity (LOH) of the *Apc* and *p53* genes was determined through the PCR amplification of dinucleotide repeat markers. DNA was isolated from microdissected tumors (diameter, 3–6 mm) and normal intestinal tissue. Control sections were stained with H&E. DNA was extracted with a RNA/DNA extraction kit (Qiagen) and subsequently used for PCR. The reaction proceeded in a total volume of 50  $\mu\text{L}$ , containing 2 U of Taq polymerase (Promega, Madison, WI), 0.5 mmol/L dNTP, 1.5 mmol/L  $\text{MgCl}_2$ , and 50 pmol of the primers. The primer sequences were obtained from the Mouse Genome Database at the Jackson Laboratory, Bar Harbor, Maine.<sup>32</sup> The following polymorphic dinucleotide repeat markers were used for the *Apc* locus (chromosome 18; 15 cM): D18Mit64 (2 cM), D18Mit111 (11 cM), D18Mit132 (11 cM), and D18Mit17 (20 cM). For the *p53* locus (chromosome 11; 39 cM), we used the following polymorphic dinucleotide repeat markers: D11Mit4 (37 cM), D11Mit30 (39.8 cM), and D11Mit278 (40 cM). The PCR products were separated on polyacrylamide gels (9%) stained in silver nitrate,<sup>33</sup> and the band intensities were quantified. Tumoral tissue was evaluated simultaneously with normal intestinal mucosa from the same animal. The ratio of the allele band intensities of tumors was divided by the corresponding ratio for normal mucosa. LOH was defined at  $P < 0.05$  for 3 independent PCR reactions.<sup>34</sup>

### Detection of p53 Mutations

A functional assay was used as described in detail by Flaman et al.<sup>35</sup> to ensure that molecular changes detected are deleterious for p53 function and, thus, true mutations.<sup>35</sup> This assay was modified for murine p53 by Ba et al.<sup>36</sup> Briefly, the functional assay is based on the fact that transcriptional activity of p53 is functional in yeast and that p53 mutants that are inactive in humans or mouse are also inactive in yeast. The

recipient yeast strain (yIG397) is defective in adenine synthesis because of a mutation in its endogenous ADE2 gene, but it contains a second copy of the ADE2 open-reading frame controlled by a p53 response promoter. Because ADE2<sup>-</sup> mutant stains grown on low-adenine plates turn red, yIG397 colonies containing mutant p53 are red, whereas colonies containing wild-type p53 are white. The yeast strain yIG397 was cotransformed with a linearized expression vector and with RT-PCR-amplified p53 from total RNA extracts from tumors. The p53 cDNA was cloned in vivo by homologous recombination. We visually quantified the percentage of red and white colonies in each assay. As previously shown, more than 10% of red colonies is always associated with a p53 mutation.<sup>37</sup> Sequencing was performed both on pooled and on individual clones to identify the mutation.

## Results

### Generation of K-ras<sup>V12G</sup> Transgenic Mice

A 9-kb regulatory region of the mouse villin gene was used to drive the selective expression of a K-ras<sup>V12G</sup> transgene in epithelial cells of the large and small intestine. We have shown earlier that the villin regulatory region targets stable and homogeneous expression of transgenes all along the crypt-villus axis, in differentiated enterocytes as well as in the immature stem cells of the crypt.<sup>22,23</sup> Villin is an actin-binding protein that is expressed in immature, as well as in differentiated intestinal and renal epithelia and also in colonic crypt stem cells.<sup>38</sup> By classical transgenesis in B6D2 mice, we have obtained 4 different founders (Fo8, Fo14, Fo33, and Fo47) that express the transgene in the small and large intestine, as evidenced by RT-PCR (Figure 1A). Three founders (Fo 8, Fo14, and Fo47) expressed the transgene also in the kidney. All founders showed germline transmission to their offspring, and the resulting animals demonstrated no obvious differences to their wild-type littermates in terms of fertility, size, and weight distribution.

### Oncogenic K-ras<sup>V12G</sup> Leads to Activation of the ERK1/2 Pathway, but Akt/PKB Is Not Activated

In tissue extracts from the intestinal mucosa of transgenic animals, the transgenic K-ras<sup>V12G</sup> was distinguishable from endogenous Ras because of its slightly altered migration in SDS-PAGE (Figure 1B, upper panel; the upper band marked by an asterisk). The expression levels were stable but rather low; the amount of transgene was quantified as  $12\% \pm 2.6\%$  of total endogenous Ras, as judged by staining with a pan-Ras antibody. To test whether the transgenic Ras protein was indeed functional in its activated, GTP-bound form in

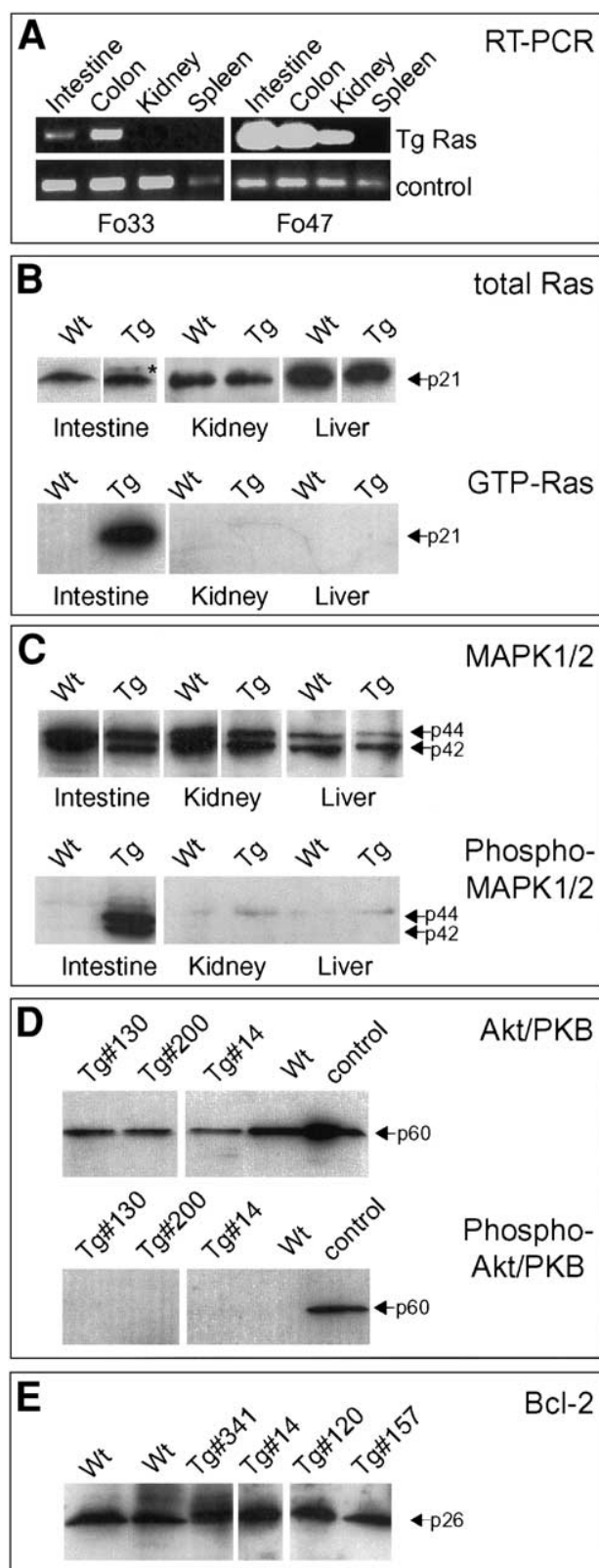


**Figure 1.** (A) Products of RT-PCR analysis revealed on an agarose gel. The 4 transgenic lines (Fo8, Fo14, Fo33, and Fo47) were tested for the tissue-specific expression of the transgene and the transcription factor TFIIID used as a control. The line Fo33 expresses the transgene in the small intestine and in the colon. The line Fo47 (as well as Fo8

and Fo14, not shown) expresses the transgene also in the kidney. (B-E) Western blots were immunostained as indicated. In B and C, tissue lysates from the transgenic line Fo47 were used. (B) *Upper panel*: Staining with a pan-Ras antibody reveals endogenous Ras proteins in tissue lysates from wild-type (Wt) littermates or transgenic mice (Tg). The transgenic *K-ras*<sup>V12G</sup> shows altered migration as compared with endogenous Ras proteins and is detectable in the intestine of transgenic animals (*asterisk*). *Lower panel*: A demonstrative Ras-GTP pull-down assay revealed with an anti-Ras antibody shows strong GTP-Ras activity in intestinal mucosa lysates of the transgenic animal. (C) *Upper panel*: Total MAPK1/2 expression levels are essentially unchanged in Tg. *Lower panel*: MAPK1/2 are clearly activated by oncogenic Ras, as revealed by a phosphospecific antibody in intestinal mucosa lysates in the transgenic animal. (D) *Upper panel*: Total Akt/PKB expression is unchanged in intestinal lysates from various transgenic animals (Tg) as compared with a Wt littermate. *Lower panel*: Activated phospho-Akt/PKB is not detectable in intestinal lysates from transgenic animals (Tg) and Wt mice (control: mouse brain lysate). (E) The expression of the antiapoptotic protein Bcl-2 is unchanged in intestinal lysates from various transgenic animals (Tg) as compared with 2 Wt littermates.

**Table 1.** Intestinal Neoplasia in K-ras<sup>V12G</sup> Mice

Genotype	Age (mo)	No. studied	No. of animals with tumors (%)	No. of tumors/animal	Tumor range	Size distribution <sup>b</sup>	Localization <sup>c</sup>
Control <sup>a</sup>	7–23	15	0	0	0	/	/
K-ras <sup>V12G</sup> (total)	2–20	41	31 (76)	2.4	0–8	59(b), 41(s)	3(P), 46(D), 44(J), 7(C)
Young animals (Fo47, Fo33)	2–6	5	1 (20)	0.2	0–1	1 (s), 47(b), 18(s)	1 (D)
Fo47	>9	15	15 (100)	4.3	1–8	4(b), 7(b), 8(s)	35(D), 29(J), 1(C)
Fo8	>9	3	3 (100)	1.3	1–2	1(b), 14(s)	4(J), 3(P), 5(D), 6(J), 1(C)
Fo14	>9	8	7 (88)	1.9	0–4		
Fo33	>9	10	5 (50)	1.3	0–5		

<sup>a</sup>Control animals: 11 wild-type B6D2 littermates and 4 animals expressing irrelevant transgenes with the same promoter construct.

<sup>b</sup>Size distribution: (s = small lesions, diameter 0.5–2 mm, b = big lesions, diameter > 2 mm).

<sup>c</sup>Localization: number of lesions found in (P) = periampullar region, (D) = duodenum, (J) = jejunum, (C) = colon.

gated for changes in its expression level. We detected no differences between transgenic and control animals (Figure 1E).

### Intestinal Neoplasia in K-ras<sup>V12G</sup> Transgenic Animals

We examined the effect of the K-ras<sup>V12G</sup> transgene expression by analyzing the intestines of mice at various stages of life. A total of 41 transgenic mice were analyzed, and 31 animals had intestinal tumors (Table 1). In addition, 11 wild-type littermates and 4 animals expressing irrelevant transgenes under control of the villin promoter were investigated. The control animals, which had the same genetic background and age distribution as the transgenic mice, were all tumor free (not shown). At 2–6 months of age, a single lesion was observed in 1 of 5 K-ras<sup>V12G</sup> transgenic animals that were analyzed (Table 1), and no ACF were detected in the colon. Older mice that passed the age of 9 months frequently had to be killed because of signs of distress and were affected by tumors in over 80% of the cases (n = 36). The average number of tumors in the small intestine was 2.5 per animal, with a range of 0 to 8 and varying sizes of up to 6 mm in diameter; sex had no influence on tumor incidence. The lesions localized to the periampullar region (3%), to the duodenum (46%), jejunum (44%), and colon (7%). Histologically, tumors corresponded to tubuloglandular adenomas or to malignant adenocarcinomas (Figure 2A–F). Adenomas presented a moderate to severe dysplasia of the epithelium. Adenocarcinoma was associated with a prominent stromal reaction and invaded the connective tissue to the muscularis mucosa or to the inner layer of muscularis

(invasive adenocarcinoma in Figure 2E and F). Mitotic features were numerous (arrow in Figure 2D). We frequently observed tumors of different sizes and stages in the same animal, an example for a smaller polypoid lesion that was present in an animal with an adenocarcinoma is shown in Figure 2G. ACF were also frequently detected in the colonic mucosa (ACF detected in all 5 animals analyzed, Figure 2H). Figure 2I and J show an example of invasive growth of tumor cells in the muscular layer; the tumor cells are of epithelial origin and can be identified with an antivillin staining. The tumor multiplicity increased in the animals in an age-dependent fashion (not shown). All 4 transgenic lines developed intestinal lesions, with differences in the severity of the phenotype (Table 1). Whereas all animals over 9 months of age had lesions in the lines Fo8 and Fo47 and 7 of 8 animals in the line Fo14, only 50% of the animals from line Fo33 developed lesions. The average tumor number per animal was different, ranging from 4 lesions/animal for line Fo47 to 1 lesion/animal for the line Fo33, with lines Fo8 and Fo14 showing intermediate numbers. These differences corresponded to the varying copy numbers of the integrated transgene, as determined by Southern blot (Fo33: 1 copy; Fo47: 5 copies; not shown). Similarly, the expression of the transgene as determined by the amount of GTP-Ras in the pull-down assay was somewhat lower in animals from the line Fo33 as compared with the other 3 lines (not shown). Interestingly, we noted the presence of large, nonneoplastic biliary cysts (10 mm in diameter) in the livers of 2 mice from the line Fo47, but, despite frequent invasive tumors, no signs of distant metastasis were observed.

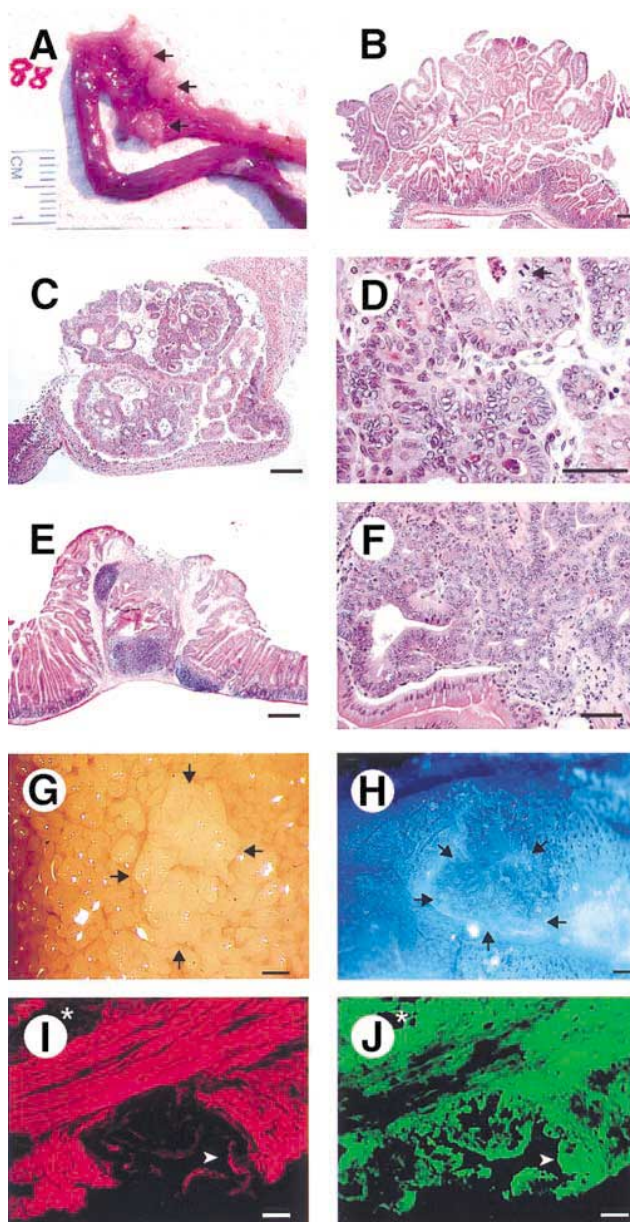


**Figure 2.** Histological analysis of representative intestinal tumors. (A) Unfixed duodenum, partly opened longitudinally, showing multiple tumors (arrows). (B–F) H&E-stained tissue sections. (B) Section of a highly dysplastic adenoma from the region visible in (A). (C) Section of an adenocarcinoma localized in the duodenum of a different animal. (D) Higher enlargement of a section of the adenocarcinoma visible in (C); the arrow denotes a mitotic figure. (E) Invasive adenocarcinoma with massive inflammation from a third animal. (F) Higher magnification of the same lesion, showing a trabecular structure of invasive epithelial cells. (G) Earlier stages of polypoid growth were also observed, often together with an adenocarcinoma in the same animal. Here, a small polyp in the duodenum (unfixed) is shown; the arrows denote the outline of the lesion. (H) Aberrant crypt focus (ACF) in the colonic epithelium. The arrows denote the enlarged, elongated crypts with thickened crypt walls. (I, J) Double immunofluorescence of an invasive adenocarcinoma in the jejunum. The asterisk denotes the luminal side of the intestine; the arrowhead points to cells of epithelial origin that grow in the muscular layer. (I) Actin filaments were stained with TRITC-phalloidin (red). (J) Cells of epithelial origin were identified with a monoclonal antivillin antibody (green). Note the apical staining for villin in the tumor cells (arrowhead) (bars = 200  $\mu$ m in B,C,G,H; 50  $\mu$ m in D,F,I,J).

### Analysis of Cell Proliferation and *Apc* Status in Intestinal Tumors

In tumors from transgenic animals, we frequently detected a strikingly disorganized cellular proliferation by immunofluorescence analysis of anti-Ki67 staining, as opposed to the highly organized and spatially restricted pattern of proliferation in normal intestinal epithelium (Figure 3A and B). This is in accordance with the high number of mitotic figures found in the histopathological analysis (Figure 2D). To investigate differences in cellular proliferation with higher precision, we analyzed normal intestinal mucosa and tumor samples by flow cytometry after in vivo BrdU incorporation (Figure 4). Quantification of the S-phase fraction (SPF) in normal mucosa showed no significant differences between wild-type (SPF: 4.1%  $\pm$  0.8%) and transgenic animals (SPF: 4.4%  $\pm$  0.4%). However, 4 of 6 tumors analyzed showed significantly elevated S-phase fractions (up to 9.2%). Although aneuploidy is a frequent feature in colorectal cancer, all tumors showed a DNA-diploid profile resembling that of normal mucosa. However, we cannot exclude that this is caused by the limits of detection of small subpopulations of cancer cells in a heterogeneous sample. We investigated whether spontaneous genetic alterations such as allelic losses were detectable in the tumors, notably for the tumor-suppressor gene *Apc*. LOH, i.e., the loss of 1 of the parental alleles present in adult cells, is a very common phenomenon in human epithelial cancers.<sup>42</sup> Furthermore, LOH of the wild-type allele of *Apc* characterizes the vast majority of intestinal tumors in several mouse models such as *Apc1638N* or *Apc $\Delta$ 716*, which carry heterozygous chain-termination mutations in the mouse *Apc* gene.<sup>43–45</sup> As a control, we analyzed intestinal tumors from *Apc1638N* mice under the same conditions as *K-ras*<sup>V12G</sup> animals, and we were able to detect LOH at the *Apc* locus in 2 of 3 tumors that were analyzed (not shown). Because the transgenic *K-ras*<sup>V12G</sup> animals were produced in the hybrid strain B6D2, they show a distribution of DBA/2 and C57Bl/6 alleles in their genome. This facilitated the analysis with polymorphic dinucleotide repeat markers. Of 11 lesions that were tested, 5 were informative in this assay. Surprisingly, none of these 5 tumors showed signs of LOH (Figure 4B). Although we did not detect LOH for the *Apc* locus, we cannot exclude the presence of somatic mutations that may in rare cases affect both alleles independently. In the cases where the LOH analysis was not informative because of homozygosity for either the DBA/2 or the C57Bl/6 allele, we have carried out  $\beta$ -cate-

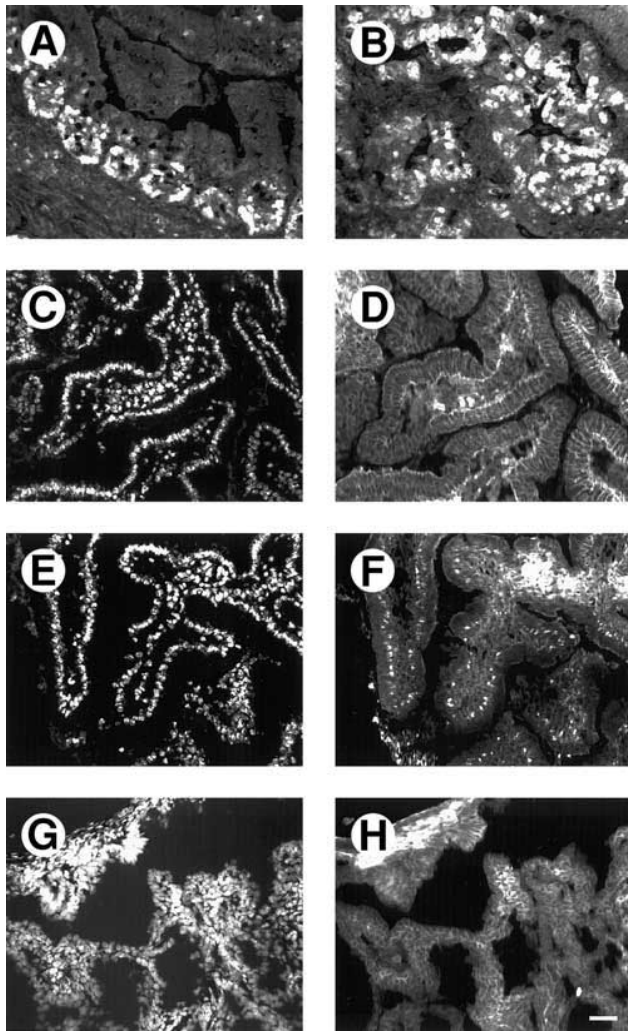


**Figure 3.** (A–H) Immunofluorescence on tissue sections. (A) Proliferating cells marked by anti-Ki67 staining are only observed in the crypts in normal intestinal tissue of a transgenic mouse. (B) Chaotic cell proliferation in an adenocarcinoma from the same animal revealed by anti-Ki67 staining. (C,E,G) Control nuclear staining with Hoechst. (D,F,H) Staining with an anti- $\beta$ -catenin antibody. (D) In normal intestinal tissue from an *Apc1638N* animal,  $\beta$ -catenin localizes to the basolateral membrane. (F) The signaling protein  $\beta$ -catenin is known to enter the nucleus upon *Apc* mutations. Indeed,  $\beta$ -catenin shows nuclear localization in an intestinal tumor section from the same *Apc1638N* animal shown in (C,D). (H) In *K-ras*<sup>V12G</sup> transgenic animals, no nuclear  $\beta$ -catenin is detectable in tumor sections;  $\beta$ -catenin localizes to the basolateral membrane in this representative section (bar = 50  $\mu$ m).

nin staining on tissue sections from tumors. The signaling molecule  $\beta$ -catenin enters the nucleus upon *Apc* mutations, which has been described for human cancer.<sup>46</sup> As a positive control, we stained tissue sections from tumors derived from *Apc1638N* animals under the same conditions and were able to detect nuclear staining (Figure 3F). In normal tissue from these mice,  $\beta$ -catenin localizes to the basolateral membrane (Figure 3D). In the

case of tumors from *K-ras*<sup>V12G</sup> transgenic animals (6 tumors tested), we found, as for the control, basolateral membrane staining for  $\beta$ -catenin in all cases observed (Figure 3H).

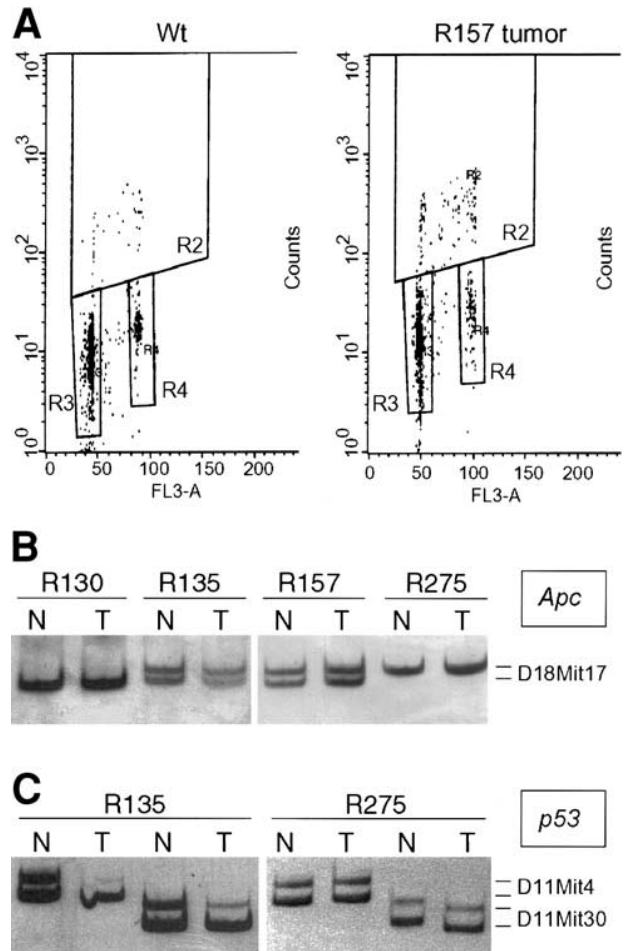


**Figure 4.** (A) Analysis of cell proliferation by cytometry after *in vivo* BrdU incorporation on intestinal mucosa from a wild-type animal (Wt; left panel) and a tumor sample from a transgenic animal (R157, right panel). Normal mucosa from the same transgenic animal did not differ significantly from the wild-type control (not shown). The bivariate histogram displays DNA content vs. BrdU incorporation. The slanting line separates the BrdU labeled and unlabeled cell populations. The vertical lines enclose the following populations: R2 corresponds to the cells in S-phase, R3 corresponds to the G0/G1-phase, and R4 to the G2/M-phase of the cell cycle. The S-phase fractions were calculated as the following: Wt: 3.1%, R157 tumor: 9.0%. (B) Representative loss of heterozygosity (LOH) analysis for the *Apc* locus, revealed on a silver-stained polyacrylamide gel. PCR was carried out in parallel on normal tissue (N) and tumor samples (T) for each transgenic animal, and the allelic ratios were compared. No LOH was observed in tumor DNA from all transgenic animals tested (here: animals R135 and R157). The analysis was not informative in several cases because of homozygosity for the dinucleotide repeat markers (e.g., animals R130 and R275 for the marker D18Mit17). (C) LOH analysis for the *p53* locus, revealed on a silver-stained polyacrylamide gel. PCR was carried out in parallel on normal tissue (N) and tumor samples (T). DNA isolated from a tumor from animal R135 shows LOH for 2 dinucleotide repeat markers (D11Mit4, D11Mit30). A different tumor sample (R275) shows no LOH.

### Analysis of the p53 Status

Mutations in the tumor-suppressor gene *p53* are a late but frequent event in human colorectal cancer. To test if this is also true for the Ras-induced tumors, we were investigating the *p53* status by LOH analysis. Two of 7 tumors showed LOH for *p53*, as evidenced by the loss of several dinucleotide markers at both sides of the *p53* locus on chromosome 11 (Figure 4C). To further assess the *p53* status for this group of tumors in an independent fashion, we used the yeast functional assay originally devised by Flaman et al.,<sup>35</sup> as modified by Ba et al.<sup>36</sup> for rodent tumors. This assay scans most of the coding region of the *p53* gene and allows the detection of mutant *p53* even in extracts from tumors with a high content in normal cells. Transcriptional activation is the critical biochemical function of *p53*, which underlies its tumor-suppressor activity. Mutant *p53* proteins fail to activate transcription. Briefly, the functional assay is based on the fact that such transcriptional activity is functional in yeast. *p53* Mutants that are inactive in humans or mouse also fail to activate transcription of a reporter gene in yeast. Normal intestinal tissue samples from transgenic animals, as well as tissue from wild-type animals were negative in this assay. Interestingly, 2 intestinal tumors derived from *Apc1638N* animals were also found negative. One of 7 tumors from *K-ras*<sup>V12G</sup> animals scored positive, giving a number of mutant yeast clones significantly higher than the background level. Subsequent sequencing of several independent clones allowed the detection of an insertion of 6 bases at codon 213 of the *p53* coding region. This insertion of 2 amino acid residues in the DNA-binding domain of the protein inactivates *p53* function. Interestingly, the tumor that carried the insertional mutation did not show LOH for the wild-type allele. However, loss of the wild-type *p53* allele is not a prerequisite for tumorigenic effects, because mutations in the heterozygous state can be sufficient, acting via a reduction of functional protein levels.<sup>47</sup> Altogether, 3 of 7 tumors derived from *K-ras*<sup>V12G</sup> transgenic animals showed an altered *p53* status: Two showed LOH for the *p53* locus, and 1 carried an insertional mutation. The same 7 tumors had also been tested for LOH at the *Apc* locus and were found negative in 5 cases; 2 were uninformative for the markers tested.

### Discussion

Earlier attempts to generate transgenic models for the role of oncogenic Ras in colorectal cancer have failed to produce neoplasms.<sup>11,20</sup> Expression of the transgene in postmitotic enterocytes was apparently not sufficient to induce cancer. We hypothesize that it is crucial to choose

a promoter that targets expression of the transgene in the rapidly proliferating undifferentiated cell population, as it has been shown in a study focusing on the Wnt pathway.<sup>48</sup> These cells remain anchored in the crypt during the normal renewal process of the intestinal mucosa; in addition, they undergo several cycles of cell division. These 2 features are necessary to accumulate the somatic mutations that are required for tumorigenesis. We have shown previously that the regulatory regions of the villin gene can target homogeneous expression of transgenes all along the crypt-villus axis.<sup>22,23</sup> In our transgenic animals, we detected the transgenic *K-ras*<sup>V12G</sup> as functional GTP-Ras oncoprotein in intestinal mucosa extracts, but the total concentration of endogenous Ras proteins was not altered (Figure 1B). The relatively low expression levels of the transgene in our transgenic model (12% of endogenous Ras) may explain the apparent absence of unwanted phenotypic side effects, besides the induction of tumorigenesis. To address the consequences of a continuous presence of GTP-Ras in the intestinal epithelium, we studied the putative changes in downstream signaling cascades. The MAP kinase cascade is involved in the transcriptional control of genes that are responsible in cell proliferation and differentiation. The expression of oncogenic Ras lead to a constitutive activation of the MAP kinases ERK1/2 in the intestinal mucosa of the transgenic animals, whereas the total expression levels remained unchanged. Interestingly, this finding bears close resemblance to the situation in human cancers. In human prostate cancer, the MAPK activity was increased 15-fold compared with control tissue, but the expression was only slightly elevated.<sup>49</sup> In colon carcinomas, the MAPK activity was reported to be significantly higher than in normal mucosa.<sup>50</sup> The protein kinase Akt/PKB is a central part of another major signaling pathway downstream of Ras, and it is generally assumed that Akt/PKB is an important effector of Ras in the tumorigenic process. Akt/PKB is a common target of the PI3-kinase, and it phosphorylates caspase-9<sup>51</sup> and the protein BAD, a member of the Bcl-2 family.<sup>52</sup> In addition to its pronounced antiapoptotic effect, Akt mediates the effects of oncogenic Ras on cell cycle progression.<sup>53</sup> Nonetheless, the tissue-specific role of Akt in Ras-mediated transformation of intestinal epithelial cells is currently under debate, based on studies of cultured cells. The expression of oncogenic H-Ras in rat intestinal epithelial cells has been reported to result in the PI3 kinase-dependent activation of Akt/PKB.<sup>54</sup> However, PI3-kinase/Akt signaling was neither necessary nor sufficient for *K-ras*-mediated transformation in the same cell type.<sup>55</sup> Interestingly, we did not observe an activa-

tion of Akt/PKB in the normal mucosa of transgenic animals. Similarly, transgenic activation of H-*ras* in neurons constitutively elevated the phosphorylation levels of MAPK (ERK1/2) but did not increase the activity of Akt/PKB.<sup>56</sup> The lack of activation of Akt/PKB and the unchanged expression of the death-suppressor Bcl-2 suggest that the regulation of apoptosis might not be affected in the intestinal mucosa of transgenic animals, at least not through these 2 key players. To test this hypothesis, we quantified the level of apoptosis with a TUNEL assay (terminal deoxynucleotidyl-transferase mediated, dUTP nick-end labeling; Boehringer Mannheim Corp.) performed on intestinal sections. We did not detect any differences between transgenic and control animals (not shown). Apparently, there is no antiapoptotic effect of oncogenic Ras in the normal mucosa of transgenic mice. Spontaneous mutations in the Akt/PKB signaling cascade may be necessary to provide an antiapoptotic effect that conveys a selective advantage for clonal expansion to tumor cells. However, when we investigated the activation of Akt/PKB and the expression levels of Bcl-2 in a number of tumors ( $n = 3$ ), we did not observe differences to normal tissue.

We detected the adenomas and malignant adenocarcinomas mainly in the duodenum and jejunum, thus in the small intestine of the transgenic animals. Nonetheless, we did not detect distant metastasis. Although we frequently found ACF in the large intestine, no malignant lesions were observed in the colon or rectum. In the human disease, most cancers arise in the large intestine.<sup>57</sup> However, the lesions frequently progress to more proximal segments of the bowel in human patients with the familial adenomatous polyposis (FAP) syndrome.<sup>58</sup> Moreover, upper gastrointestinal lesions such as duodenal adenomas are frequently found in attenuated forms of FAP.<sup>59</sup> Tumor analysis by flow cytometry showed that a majority of the lesions were hyperproliferative, but overall all lesions tested appeared diploid. Given the fact that aneuploidy is a common factor in intestinal cancer,<sup>42</sup> we cannot exclude the presence of subtle genetic alterations that may not be detectable by flow cytometry. The normal mucosa of transgenic animals had essentially unchanged populations of S-phase cells, when compared with wild-type littermates. In line with this, activation of Ras was reported to promote progression throughout G<sub>1</sub>, but not S phase, in premalignant lesions.<sup>60</sup> However, the S-phase fractions were elevated up to 2-fold in several tumors. This finding implies that the constitutive activation of the MAPK cascade that we observed in normal mucosa was not sufficient to increase the rate of cellular proliferation. Additional genetic alterations are most

likely required to unbalance the tightly controlled system of cell number homeostasis in the intestinal epithelium, such as is the case for the human disease. The spontaneous alterations that seem to be required for tumor progression are rare and rate-limiting events, because the lesions in our model develop at moderate numbers (2.4 per animal) and with a relatively late onset (>6 months, at this age the *Apc1638N* mice already begin to die because of high cancer load<sup>4</sup>). Because *Apc* is known as the "gatekeeper" in intestinal epithelial proliferation and plays a crucial role in human colorectal cancer development, we set out to investigate a putative inactivation of this gene. Moreover, although K-*ras* mutations are found in early to intermediate stages of cancer development, it is generally assumed that their tumorigenic effects develop in the context of a preexisting *APC* gene mutation.<sup>13,15,21</sup> Strikingly, we did not obtain evidence for inactivation of the *Apc* gene in all the tumors that were analyzed by different methods ( $n = 11$ ). Murine intestinal tumors in the absence of mutations in *Apc* or  $\beta$ -catenin have also been reported for a recent mouse model that investigates the role of the transforming growth factor  $\beta$  pathway.<sup>61</sup>

As Fearon and Vogelstein et al.<sup>13</sup> stated, mutated K-*ras* may either be the initiating event in some colorectal tumors or rather depend on previous *APC* mutations in colorectal cancer cells to exert their oncogenic effects. Recent results from human primary carcinomas that arise in the small intestine indicate that *ras* is frequently mutated (in 53% of the cases), *p53* to a lesser extent (27%), whereas *APC* mutations occurred at a very low frequency (6%).<sup>62</sup> A recent study investigated the mutational status of ACF, which are putative early precursor lesions of colorectal cancer. Two main types of ACF have been described for human colon mucosa: nondysplastic ACF that are associated with *ras* mutations and dysplastic ACF that are associated with *APC* mutations and that are considered to be more likely to progress to adenoma.<sup>63</sup> However, it appears that only a small fraction of the ACF progresses to large polyps, let alone tumors. A recent study found frequent K-*ras* mutations in ACF (in 80% of nondysplastic and in more than 60% of dysplastic ACF), but no evidence for *APC* or  $\beta$ -catenin mutations was obtained.<sup>64</sup> According to the authors, there seems to be a route to sporadic colorectal cancer where K-*ras* mutations occur very early during the formation of precursor lesions, which then progress to adenomas, where further mutations take place.<sup>64</sup> Because *Apc* seemed not to be required for tumorigenesis in the transgenic animals, we wanted to study the putative changes in the status of the tumor-suppressor gene *p53*.

Indeed, 3 of 7 lesions displayed an altered *p53* state. Two lesions showed LOH at the *p53* locus on chromosome 11; in addition, we detected in 1 tumor an inactivating *p53* mutation in the *p53* reading frame. Thus, spontaneous mutation of *p53* is a frequent but nonexclusive feature in tumors arising in the *K-ras*<sup>V12G</sup> transgenic animals, matching the genetic situation in human colorectal cancer. An inactivation of *p53* could shift the balance of cell proliferation vs. apoptosis toward proliferation, thus conveying a selective growth advantage to mutated cells. Furthermore, recent findings indicate a cross talk between oncogenic Ras and the *p53* pathway.<sup>65</sup> The protein Mdm2, one of the major regulators of *p53*, as well as its inhibitor p19<sup>ARF</sup> have been shown to be a target of the Ras/Raf/MAP kinase pathway.<sup>66</sup> Further investigation will be necessary to elucidate the nature of the putative cooperation between *K-ras* and *p53* in this model. Additional key players in tumorigenesis apart from *p53* that either aggravate the effects of oncogenic Ras or act via independent pathways might also be identified with the help of this mouse model. However, *p53* mutations are very rare in the case of *Apc*-induced intestinal lesions in mice. Neither in the *Apc1638N*<sup>45</sup> nor in the *Min* mouse<sup>67</sup> have spontaneous *p53* alterations been detected. Interestingly, combinations of *Min* or *Apc1638N* mice with knockout mutants for *p53* did not lead to increased tumor formation in the gastrointestinal tract.<sup>68,69</sup> Taken together, this indicates that the inactivation of *p53* is not required in the case of *Apc*-induced tumorigenesis in mice. However, one has to keep in mind that both Ras and *p53* do not act in a completely separate fashion from the Wnt/APC pathway. Recent evidence shows that there are several interconnections between the signaling cascades. The protein glycogen synthase kinase 3 is not only a component of the Wnt/Wingless pathway but it is also a substrate of Ras-activated PKB that is capable of down-regulating its activity.<sup>16</sup> Another example is the Myc protein: It is stabilized by Ras,<sup>70</sup> and the transcription of *myc* is induced by the  $\beta$ -catenin pathway.<sup>71</sup> Furthermore, oncogenic  $\beta$ -catenin has been shown to induce accumulation and activation of the *p53* tumor-suppressor protein.<sup>72</sup> Interestingly, a recent murine model for Ras-dependent carcinogenesis based upon rare spontaneous recombination events failed to develop intestinal lesions, despite the presence of tumors in other tissues.<sup>12</sup> This could be interpreted as an indication that oncogenic Ras is not able to induce tumors in the intestine. However, tumorigenesis is a rare event even in our transgenic animals, which express oncogenic Ras throughout the intestinal epithelium. If one assumes that the number of cells that express oncogenic Ras in the model described

by Johnson et al.<sup>12</sup> is strongly reduced as compared with our transgenic model, the probability to acquire additional spontaneous mutations (e.g., LOH of *p53*) might simply be too low to induce tumorigenesis in their case. Altogether, our animal model recapitulates histopathologic as well as genetic features of the human disease, and it displays a close resemblance to the stages of tumor progression in human colorectal cancer, ranging from preinvasive precursor lesions to invasive adenocarcinoma. Our results underline the notion that the pathway to colon cancer is not necessarily a single road. Furthermore, they indicate that inactivation of the tumor-suppressor gene *p53* seems to cooperate with *K-ras* in the progression of colorectal tumors.

## References

1. Kinzler KW, Vogelstein B. Lessons from hereditary colorectal cancer. *Cell* 1996;87:159–170.
2. Heyer J, Yang K, Lipkin M, Edelmann W, Kucherlapati R. Mouse models for colorectal cancer. *Oncogene* 1999;18:5325–5333.
3. Su LK, Kinzler KW, Vogelstein B, Preisinger AC, Moser AR, Luongo C, Gould KA, Dove WF. Multiple intestinal neoplasia caused by a mutation in the murine homolog of the APC gene. *Science* 1992; 256:668–670.
4. Fodde R, Edelmann W, Yang K, van Leeuwen C, Carlson C, Renault B, Breukel C, Alt E, Lipkin M, Khan PM, Kucherlapati R. A targeted chain-termination mutation in the mouse *Apc* gene results in multiple intestinal tumors. *Proc Natl Acad Sci U S A* 1994;91:8969–8973.
5. Bienz M, Clevers H. Linking colorectal cancer to Wnt signaling. *Cell* 2000;103:311–320.
6. de Wind N, Dekker M, Berns A, Radman M, te Riele H. Inactivation of the mouse *Msh2* gene results in mismatch repair deficiency, methylation tolerance, hyperrecombination, and predisposition to cancer. *Cell* 1995;82:321–330.
7. Edelmann W, Cohen PE, Kane M, Lau K, Morrow B, Bennett S, Umar A, Kunkel T, Cattoretti G, Chaganti R, Pollard JW, Kolodner RD, Kucherlapati R. Meiotic pachytene arrest in *MLH1*-deficient mice. *Cell* 1996;85:1125–1134.
8. Zhu Y, Richardson JA, Parada LF, Graff JM. *Smad3* mutant mice develop metastatic colorectal cancer. *Cell* 1998;94:703–714.
9. Sasaki T, Irie-Sasaki J, Horie Y, Bachmaier K, Fata JE, Li M, Suzuki A, Bouchard D, Ho A, Redston M, Gallinger S, Khokha R, Mak TW, Hawkins PT, Stephens L, Scherer SW, Tsao M, Penninger JM. Colorectal carcinomas in mice lacking the catalytic subunit of PI(3)K $\gamma$ . *Nature* 2000;406:897–902.
10. Barbier M, Attoub S, Calvez R, Laffargue M, Jarry A, Mareel M, Altruda F, Gespach C, Wu D, Lu B, Hirsch E, Wymann MP. Tumour biology. Weakening link to colorectal cancer? *Nature* 2001;413: 796.
11. Coopersmith CM, Chandrasekaran C, McNeven MS, Gordon JL. Bi-transgenic mice reveal that *K-ras*Val12 augments a *p53*-independent apoptosis when small intestinal villus enterocytes reenter the cell cycle. *J Cell Biol* 1997;138:167–179.
12. Johnson L, Mercer K, Greenbaum D, Bronson RT, Crowley D, Tuveson DA, Jacks T. Somatic activation of the *K-ras* oncogene causes early onset lung cancer in mice. *Nature* 2001;410:1111–1116.
13. Bos JL, Fearon ER, Hamilton SR, Verlaan-de Vries M, van Boom JH, van der Eb AJ, Vogelstein B. Prevalence of *ras* gene mutations in human colorectal cancers. *Nature* 1987;327:293–297.
14. Forrester K, Almoguera C, Han K, Grizzle WE, Perucho M. Detec-

- tion of high incidence of *K-ras* oncogenes during human colon tumorigenesis. *Nature* 1987;327:298–303.
15. Fearon ER, Vogelstein B. A genetic model for colorectal tumorigenesis. *Cell* 1990;61:759–767.
  16. McCormick F. Signalling networks that cause cancer. *Trends Cell Biol* 1999;9:M53–M56.
  17. Gire V, Marshall CJ, Wynford-Thomas D. Activation of mitogen-activated protein kinase is necessary but not sufficient for proliferation of human thyroid epithelial cells induced by mutant Ras. *Oncogene* 1999;18:4819–4832.
  18. Gire V, Marshall C, Wynford-Thomas D. PI-3-kinase is an essential anti-apoptotic effector in the proliferative response of primary human epithelial cells to mutant RAS. *Oncogene* 2000;19:2269–2276.
  19. Shields JM, Pruitt K, McFall A, Shaub A, Der CJ. Understanding Ras: “it ain’t over ‘til it’s over.” *Trends Cell Biol* 2000;10:147–154.
  20. Kim SH, Roth KA, Moser AR, Gordon JI. Transgenic mouse models that explore the multistep hypothesis of intestinal neoplasia. *J Cell Biol* 1993;123:877–893.
  21. Yamashita N, Minamoto T, Ochiai A, Onda M, Esumi H. Frequent and characteristic *K-ras* activation in aberrant crypt foci of colon. Is there preference among *K-ras* mutants for malignant progression? *Cancer* 1995;75:1527–1533.
  22. Robine S, Jaisser F, Louvard D. Epithelial cell growth and differentiation. IV. Controlled spatiotemporal expression of transgenes: new tools to study normal and pathological states. *Am J Physiol* 1997;273:G759–G762.
  23. Pinto D, Robine S, Jaisser F, El Marjou FE, Louvard D. Regulatory sequences of the mouse villin gene that efficiently drive transgenic expression in immature and differentiated epithelial cells of small and large intestines. *J Biol Chem* 1999;274:6476–6482.
  24. McCoy MS, Bargmann CI, Weinberg RA. Human colon carcinoma *Ki-ras2* oncogene and its corresponding proto-oncogene. *Mol Cell Biol* 1984;4:1577–1582.
  25. Costa de Beauregard MA, Pringault E, Robine S, Louvard D. Suppression of villin expression by antisense RNA impairs brush border assembly in polarized epithelial intestinal cells. *EMBO J* 1995;14:409–421.
  26. Laemmli UK. Cleavage of structural proteins during the assembly of the head of bacteriophage T4. *Nature* 1970;227:680–685.
  27. Towbin H, Staehelin T, Gordon J. Electrophoretic transfer of proteins from polyacrylamide gels to nitrocellulose sheets: procedure and some applications. *Proc Natl Acad Sci U S A* 1979;76:4350–4354.
  28. Dudouet B, Robine S, Huet C, Sahuquillo-Merino C, Blair L, Coudrier E, Louvard D. Changes in villin synthesis and subcellular distribution during intestinal differentiation of HT29-18 clones. *J Cell Biol* 1987;105:359–369.
  29. Smits R, Ruiz JT, Diaz-Cano S, Luz A, Jagmohan-Changur S, Breukel C, Birchmeier C, Birchmeier W, Fodde R. E-cadherin and adenomatous polyposis coli mutations are synergistic in intestinal tumor initiation in mice. *Gastroenterology* 2000;119:1045–1053.
  30. Pretlow TP, Barrow BJ, Ashton WS, O’Riordan MA, Pretlow TG, Jurcisek JA, Stellato TA. Aberrant crypts: putative preneoplastic foci in human colonic mucosa. *Cancer Res* 1991;51:1564–1567.
  31. Hamilton SR, Aaltonen, LA. WHO classification of tumours: pathology and genetics of tumours of the digestive system. Lyon: IARC Press, 2000.
  32. Blake JA, Eppig JT, Richardson JE, Bult CJ, Kadin JA. The mouse genome database (MGD): integration nexus for the laboratory mouse. *Nucleic Acids Res* 2001;29:91–94.
  33. Bamba M, Sugihara H, Okada K, Bamba T, Hattori T. Clonal analysis of superficial depressed-type gastric carcinoma in humans. *Cancer* 1998;83:867–875.
  34. Zauber NP, Sabbath-Solitare M, Marotta SP, Zauber AG, Bishop DT. Molecular changes in the *K-ras* and APC genes in colorectal adenomas and carcinomas arising in the same patient. *J Pathol* 2001;193:303–309.
  35. Flaman JM, Frebourg T, Moreau V, Charbonnier F, Martin C, Chappuis P, Sappino AP, Limacher IM, Bron L, Benhattar J, Tada M, Van Meir EG, Estreicher A, Iggo RD. A simple p53 functional assay for screening cell lines, blood, and tumors. *Proc Natl Acad Sci U S A* 1995;92:3963–3967.
  36. Ba Y, Tonoki H, Tada M, Nakata D, Hamada J, Moriuchi T. Transcriptional slippage of p53 gene enhanced by cellular damage in rat liver: monitoring the slippage by a yeast functional assay. *Mutat Res* 2000;447:209–220.
  37. de Cremoux P, Salomon AV, Liva S, Dendale R, Bouchind’homme B, Martin E, Sastre-Garau X, Magdelenat H, Fourquet A, Soussi T. p53 mutation as a genetic trait of typical medullary breast carcinoma. *J Natl Cancer Inst* 1999;91:641–643.
  38. Maunoury R, Robine S, Pringault E, Leonard N, Gaillard JA, Louvard D. Developmental regulation of villin gene expression in the epithelial cell lineages of mouse digestive and urogenital tracts. *Development* 1992;115:717–728.
  39. van der Geer P, Henkemeyer M, Jacks T, Pawson T. Aberrant Ras regulation and reduced p190 tyrosine phosphorylation in cells lacking p120-Gap. *Mol Cell Biol* 1997;17:1840–1847.
  40. Kim HA, Rosenbaum T, Marchionni MA, Ratner N, DeClue JE. Schwann cells from neurofibromin deficient mice exhibit activation of p21ras, inhibition of cell proliferation, and morphological changes. *Oncogene* 1995;11:325–335.
  41. Liu YZ, Boxer LM, Latchman DS. Activation of the Bcl-2 promoter by nerve growth factor is mediated by the p42/p44 MAPK cascade. *Nucleic Acids Res* 1999;27:2086–2090.
  42. Thiagalingam S, Laken S, Willson JK, Markowitz SD, Kinzler KW, Vogelstein B, Lengauer C. Mechanisms underlying losses of heterozygosity in human colorectal cancers. *Proc Natl Acad Sci U S A* 2001;98:2698–2702.
  43. Fodde R, Losekoot M. Mutation detection by denaturing gradient gel electrophoresis (DGGE). *Hum Mutat* 1994;3:83–94.
  44. Oshima M, Oshima H, Kitagawa K, Kobayashi M, Itakura C, Taketo M. Loss of *Apc* heterozygosity and abnormal tissue building in nascent intestinal polyps in mice carrying a truncated *Apc* gene. *Proc Natl Acad Sci U S A* 1995;92:4482–4486.
  45. Smits R, Kartheuser A, Jagmohan-Changur S, Leblanc V, Breukel C, de Vries A, van Kranen H, van Krieken JH, Williamson S, Edelmann W, Kucherlapati R, Khan PM, Fodde R. Loss of *Apc* and the entire chromosome 18 but absence of mutations at the *Ras* and *Tp53* genes in intestinal tumors from *Apc1638N*, a mouse model for *Apc*-driven carcinogenesis. *Carcinogenesis* 1997;18:321–327.
  46. Inomata M, Ochiai A, Akimoto S, Kitano S, Hirohashi S. Alteration of  $\beta$ -catenin expression in colonic epithelial cells of familial adenomatous polyposis patients. *Cancer Res* 1996;56:2213–2217.
  47. Venkatachalam S, Shi YP, Jones SN, Vogel H, Bradley A, Pinkel D, Donehower LA. Retention of wild-type p53 in tumors from p53 heterozygous mice: reduction of p53 dosage can promote cancer formation. *EMBO J* 1998;17:4657–4667.
  48. Harada N, Tamai Y, Ishikawa T, Sauer B, Takaku K, Oshima M, Taketo MM. Intestinal polyposis in mice with a dominant stable mutation of the  $\beta$ -catenin gene. *EMBO J* 1999;18:5931–5942.
  49. Price DT, Rocca GD, Guo C, Ballo MS, Schwinn DA, Luttrell LM. Activation of extracellular signal-regulated kinase in human prostate cancer. *J Urol* 1999;162:1537–1542.
  50. Ostrowski J, Trzeciak L, Kolodziejcki J, Bomsztyk K. Increased constitutive activity of mitogen-activated protein kinase and re-naturable 85 kDa kinase in human-colorectal cancer. *Br J Cancer* 1998;78:1301–1306.
  51. Cardone MH, Roy N, Stennicke HR, Salvesen GS, Franke TF, Stanbridge E, Frisch S, Reed JC. Regulation of cell death pro-

- tease caspase-9 by phosphorylation. *Science* 1998;282:1318–1321.
52. Datta SR, Dudek H, Tao X, Masters S, Fu H, Gotoh Y, Greenberg ME. Akt phosphorylation of BAD couples survival signals to the cell-intrinsic death machinery. *Cell* 1997;91:231–241.
  53. Gille H, Downward J. Multiple ras effector pathways contribute to G(1) cell cycle progression. *J Biol Chem* 1999;274:22033–22040.
  54. Sheng H, Shao J, DuBois RN. Akt/PKB activity is required for Ha-Ras-mediated transformation of intestinal epithelial cells. *J Biol Chem* 2001;276:14498–14504.
  55. McFall A, Ulku A, Lambert QT, Kusa A, Rogers-Graham K, Der CJ. Oncogenic Ras blocks anoikis by activation of a novel effector pathway independent of phosphatidylinositol 3-kinase. *Mol Cell Biol* 2001;21:5488–5499.
  56. Heumann R, Goemans C, Bartsch D, Lingenhohl K, Waldmeier PC, Hengerer B, Allegrini PR, Schellander K, Wagner EF, Arendt T, Kamdem RH, Obst-Pernberg K, Narz F, Wahle P, Berns H. Transgenic activation of Ras in neurons promotes hypertrophy and protects from lesion-induced degeneration. *J Cell Biol* 2000;151:1537–1548.
  57. Powell SM, Zilz N, Beazer-Barclay Y, Bryan TM, Hamilton SR, Thibodeau SN, Vogelstein B, Kinzler KW. APC mutations occur early during colorectal tumorigenesis. *Nature* 1992;359:235–237.
  58. Buflin JA. Colorectal cancer genetics. Closing the gap between genotype and phenotype. *Cancer* 1995;76:2389–2392.
  59. Lynch HT, Smyrk T, McGinn T, Lanspa S, Cavalieri J, Lynch J, Slominski-Castor S, Cayouette MC, Priluck I, Luce MC. Attenuated familial adenomatous polyposis (AFAP). A phenotypically and genotypically distinctive variant of FAP. *Cancer* 1995;76:2427–2433.
  60. Wagner M, Greten FR, Weber CK, Koschnick S, Mattfeldt T, Deppert W, Kern H, Adler G, Schmid RM. A murine tumor progression model for pancreatic cancer recapitulating the genetic alterations of the human disease. *Genes Dev* 2001;15:286–293.
  61. Engle SJ, Hoying JB, Boivin GP, Ormsby I, Gartside PS, Doetschman T. Transforming growth factor beta1 suppresses nonmetastatic colon cancer at an early stage of tumorigenesis. *Cancer Res* 1999;59:3379–3386.
  62. Arai M, Shimizu S, Imai Y, Nakatsuru Y, Oda H, Oohara T, Ishikawa T. Mutations of the Ki-ras, p53 and APC genes in adenocarcinomas of the human small intestine. *Int J Cancer* 1997;70:390–395.
  63. Jen J, Powell SM, Papadopoulos N, Smith KJ, Hamilton SR, Vogelstein B, Kinzler KW. Molecular determinants of dysplasia in colorectal lesions. *Cancer Res* 1994;54:5523–5526.
  64. Takayama T, Ohi M, Hayashi T, Miyaniishi K, Nobuoka A, Nakajima T, Satoh T, Takimoto R, Kato J, Sakamaki S, Niitsu Y. Analysis of K-ras, APC, and  $\beta$ -catenin in aberrant crypt foci in sporadic adenoma, cancer, and familial adenomatous polyposis. *Gastroenterology* 2001;121:599–611.
  65. Lin AW, Lowe SW. Oncogenic ras activates the ARF-p53 pathway to suppress epithelial cell transformation. *Proc Natl Acad Sci U S A* 2001;98:5025–5030.
  66. Ries S, Biederer C, Woods D, Shifman O, Shirasawa S, Sasazuki T, McMahon M, Oren M, McCormick F. Opposing effects of Ras on p53: transcriptional activation of mdm2 and induction of p19ARF. *Cell* 2000;103:321–330.
  67. Haines J, Dunford R, Moody J, Ellender M, Cox R, Silver A. Loss of heterozygosity in spontaneous and X-ray-induced intestinal tumors arising in F1 hybrid min mice: evidence for sequential loss of APC(+) and Dpc4 in tumor development. *Genes Chromosom Cancer* 2000;28:387–394.
  68. Clarke AR, Cummings MC, Harrison DJ. Interaction between murine germline mutations in p53 and APC predisposes to pancreatic neoplasia but not to increased intestinal malignancy. *Oncogene* 1995;11:1913–1920.
  69. Smits R, van der Houven, van Oordt W, Luz A, Zurcher C, Jagmohan-Changur S, Breukel C, Khan PM, Fodde R. Apc1638N: a mouse model for familial adenomatous polyposis-associated desmoid tumors and cutaneous cysts. *Gastroenterology* 1998;114:275–283.
  70. Sears R, Leone G, DeGregori J, Nevins JR. Ras enhances Myc protein stability. *Mol Cell* 1999;3:169–179.
  71. He TC, Sparks AB, Rago C, Hermeking H, Zawel L, da Costa LT, Morin PJ, Vogelstein B, Kinzler KW. Identification of c-MYC as a target of the APC pathway. *Science* 1998;281:1509–1512.
  72. Damalas A, Kahan S, Shtutman M, Ben-Ze'ev A, Oren M. Deregulated  $\beta$ -catenin induces a p53- and ARF-dependent growth arrest and cooperates with Ras in transformation. *EMBO J* 2001;20:4912–4922.

---

Received March 22, 2002. Accepted April 15, 2002.

Address requests for reprints to: Sylvie Robine, Ph.D., CNRS-UMR144, Institut Curie, 26 rue d'Ulm, 75248 Paris Cedex 05, France. e-mail: sylvie.robine@curie.fr; fax: (33) 1-4234-6377.

Supported by grants from the Association pour la Recherche contre le Cancer (ARC; to S.R.) and the Deutsche Forschungsgemeinschaft (DFG; to K.-P.J.).

The authors thank Dr. Georges Gaudriault for the bacterial extracts containing recombinant RalGDS-GST, Dr. Philippe Vielh for allowing us to carry out the cytometry studies in his laboratory, Dr. Zofia Maciorowski for advice on cytometry, Dr. Jens Niewoehner for his help in constructing the K-ras<sup>V12G</sup> vector, Dr. Mitsuhiro Tada for providing the mouse FASAY, Dr. Riccardo Fodde for generously providing the Apc1638N mouse strain, Reeta Holmila for assistance with the FASAY, and Louis Aussepe for assistance in the animal facility.